Available online at www.sciencedirect.com

ScienceDirect

Catalysis Today 129 (2007) 169–176

CATALYSIS TODAY

www.elsevier.com/locate/cattod

Reaction intermediates and pathways in the photoreduction of oxygen molecules at the (1 0 1) TiO_2 (anatase) surface

Francesco Filippone [a,*], Giuseppe Mattioli [b,a], Aldo Amore Bonapasta [a]

[a] *Istituto di Struttura della Materia, Consiglio Nazionale delle Ricerche, Via Salaria km 29.5, CP 10, 00016 Monterotondo Stazione, Roma, Italy*
[b] *Universita degli Studi di Roma "La Sapienza", Piazzale Aldo Moro 5, 00185 Roma, Italy*

Abstract

Ab initio density functional calculations in the local spin density and Hubbard U approximations have been performed to investigate the formation of some important intermediates of the O_2 photoreduction at the (1 0 1) TiO_2 anatase surface as well as to compare with previous local density approximation results. A recently proposed approach has been used where molecules on the surface are treated like surface defects. Thus, by applying theoretical methods generally used in the physics of semiconductors, we successfully estimate the location and donor–acceptor character of the electronic levels induced by an adsorbed molecule in the TiO_2 energy gap, both crucial for the surface-molecule charge-transfer processes, and investigate the formation and the vibrational properties of charged intermediates. Present results confirm the key role played by charged intermediates in the O_2 photoreduction as well as a strong, deep acceptor character of an adsorbed O_2 molecule which gives a clear theoretical explanation of the O_2 electron scavenger behavior suggested by the experiment. Moreover, an investigation of the vibrational properties of some surface intermediates performed by *ab initio* molecular dynamics methods confirms an important role of H bonds forming between surface species and their water solvation shells.

Keywords: Titanium dioxide; Photocatalyst; Density Functional Theory

1. Introduction

Titanium dioxide is an extremely promising photocatalyst for environmental applications like the photooxidation of organic and small inorganic molecules in polluted air and water [1–6]. In general, photocatalytic processes may be roughly described in terms of the following steps: (i) adsorption of a molecule on a semiconductor surface, (ii) photogeneration of electron–hole (e–h) pairs by light irradiation, (iii) trapping of electrons (holes) at surface sites, (iv) redox processes induced by e and h transfers from the surface to adsorbed molecules. Some of these steps may crucially depend on reaction intermediates forming at the TiO_2 surface. For instance, O_2 molecules are believed to be very efficient electron scavengers. This suggests the formation of negatively charged O_2-related intermediates which prevent undesired e–h recombination and affect the step (iii) above. Furthermore, O_2-derived intermediates can induce the formation of oxidizing species responsible of the oxidation of organic compounds, thus affecting the step (iv) above [1–6]. As a matter of fact, O_2 molecules play an important role in the photocatalytic processes, being the species mainly involved in the photoreduction processes accompanying the photooxidation ones. The O_2 photoreduction in aqueous solutions in contact with UV-irradiated TiO_2 rutile or anatase nanoparticles has been investigated in a recent multiple internal reflection infrared spectroscopy (MIRIR) study [7]. In that study, observed vibrational frequencies have been assigned to primary intermediates of the O_2 photoreduction and reaction pathways have been proposed, see Fig. 1.

In a previous paper, we have investigated the properties of some intermediates of the O_2 photoreduction process by using *ab initio* density functional theory (DFT) methods in the local density approximation (LDA) and compared the theoretical results with those of the MIRIR study [8]. A recently proposed approach was used where molecules on a TiO_2 surface are treated like surface defects and investigated in the theoretical framework successfully used for defects in semiconductors

---

* Corresponding author. Tel.: +39 0690672836; fax: +39 0690672316.
E-mail address: francesco.filippone@ism.cnr.it (F. Filippone).

0920-5861/$ – see front matter © 2007 Elsevier B.V. All rights reserved.
doi:10.1016/j.cattod.2007.06.064

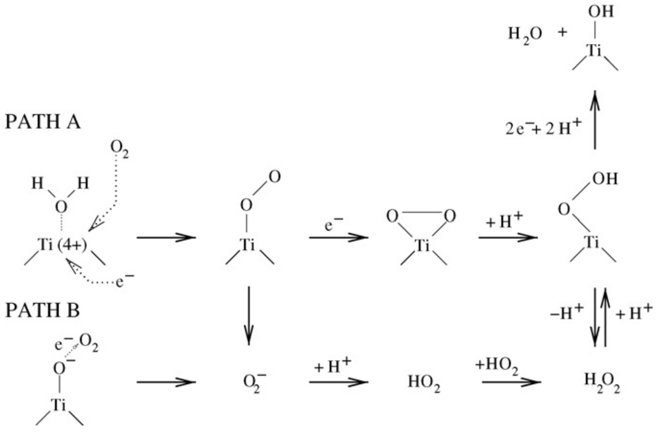

Fig. 1. Reaction pathways for the O_2 photoreduction as proposed in the MIRIR study (Ref. [7]).

[9,10]. For a given adsorbed molecule, such an approach permits to integrate in a consistent picture results concerning: (i) the strength of the surface–molecule interaction; (ii) the electronic properties of the surface–molecule system considered as a whole; (iii) the charge-transfer processes; (iv) the formation of neutral and charged intermediates; and (v) the vibrational properties of both neutral and charged species. The properties of possible intermediates were investigated in the case of the stable (1 0 1) TiO_2 anatase surface [11], that should be abundant in the anatase nanoparticles investigated in the MIRIR study. The results of that study have indicated a key role of charged intermediates in the O_2 photoreduction process as well as revealed important effects of water molecules on the vibrational properties of the surface species.

In the present study, we have further investigated the properties of some important intermediates of the same process, that is, the O_2 peroxo and hydroperoxo groups and surface OH groups and compared previous results with the present ones in order to confirm and strengthen the theoretical picture given by the LDA results. In detail, in the case of O_2 peroxo and hydroperoxo groups, we have performed local spin density (LSD) calculations in order to take into account the effects of high-spin configurations. This is motivated by the importance of such configurations in the ground state of the isolated O_2 molecule (of course, an LDA approach is a fundamentally incorrect treatment of the O_2 molecule) and possibly in the electronic states of O_2 derived surface groups. In the case of the surface OH groups, we have used a local density Hubbard U (LDA + U) approach [12] in order to investigate a possible localization of the corresponding electronic charge, as suggested by a recent theoretical study [13]. Finally, the vibrational properties of the intermediates have been here investigated both in the harmonic approximation and by performing *ab initio* molecular dynamics calculations, in which case a larger solvation shell of water molecules has been employed. This, in order to better describe the effects of temperature and hydrogen bonds on the vibrational properties of the surface species. Moreover, here we have carefully considered the charge transfer processes leading to the formation of the above intermediates. By founding on some peculiarities of the present approach, which permits to estimate the location of the electronic levels induced by an adsorbed molecule in the energy gap of the semiconductor as well as the predominant charge state of the molecule for a given position of the Fermi energy, we have discussed the formation of a charged intermediate by relating its donor/acceptor character to the effects of UV irradiation as well as of a p or n-type doping of the semiconductor. The formation of charged intermediates and the corresponding vibrational properties have been also related to the observed vibrational lines as well as to possible reaction pathways.

2. Methods

Total energies, equilibrium geometries and adsorption (desorption) enthalpies of different surface–molecule systems have been calculated by using DFT methods in the generalized gradient corrected LSD approximation [14,15] with the PBE exchange and correlation functional [16], in the supercell approach. Further calculations have been performed by using an LDA + U approach [12]. Ultrasoft pseudopotentials have been used for oxygen and titanium [17,18]. All calculations have been performed at the Γ point of the Brillouin zone. The supercells used to simulate molecules interacting with the (1 0 1) anatase surface have been obtained by adding ≈ 7 Å of empty space to a bulk 72-atom supercell containing four (2 × 3) atomic layers. Geometry optimization procedures have been performed by fully relaxing the positions of all of the atoms of a supercell, except for the atoms of the fourth layer (formed by the lowest 12 O atoms and 6 Ti atoms) which have been kept fixed to their optimized bulk positions.

Total energy values have been used to estimate the strength of a molecule–surface interaction through the calculation of desorption enthalpies, e.g., in the case of an O_2 molecule:

$$\Delta H_{(\text{des})}(O_2) = E(O_2/\text{surf}) - E(\text{surf}) - E(O_2)$$

where the total energy values are relative to supercells simulating an O_2 molecule interacting with the anatase surface, the surface, and an isolated O_2 molecule in the vacuum, respectively. ΔH values of charged species have been evaluated by including in the supercell an ancillary ionic species not interacting with the surface and having a charge opposite to that of the investigated surface species. This permits to calculate ΔH values by using neutral supercells. The ancillary species does not affect the results achieved for the structural, electronic and vibrational properties of the surface species investigated in charged supercells. A careful analysis of the electronic properties of a molecule–surface system has been performed by investigating electronic eigenvalues at the Γ point, defect formation energies and transition energy levels [9,19,20]. The two last quantities involve both neutral and charged systems and permit to estimate the location in the anatase energy gap and the character (donor or acceptor) of the electronic levels induced by an adsorbed molecule, both playing a key role in the charge transfer processes.

In a supercell approach, the formation energy $\Omega(M^q_{\mathrm{ads}})$ of an adsorbed M_{ads} molecule carrying a q charge is estimated like that of a defect by:

$$\Omega(M^q_{\mathrm{ads}}) = E(M^q_{\mathrm{ads}}) - E(\mathrm{surf}) - \mu_{\mathrm{M}} + q(\mu_{\mathrm{F}} + E_{\mathrm{VB}})$$

where $E(M^q_{\mathrm{ads}})$ and $E(\mathrm{surf})$ are the total energies of a supercell simulating a TiO_2 surface with and without a charged absorbed molecule M^q_{ads}, respectively, μ_{M} is the free-molecule chemical potential, assumed equal to the energy of one M molecule in the vacuum, and q is the negative (positive) charge on the M_{ads}, i.e. the number of electrons transferred to (from) the molecule from (to) an electron reservoir with a chemical potential, namely, a Fermi level, μ_{F}. A value of $\mu_{\mathrm{F}} = 0$ corresponds to the valence band maximum (VBM) of bulk anatase. This choice requires to explicitly include also the energy of VBM, E_{VB}, in the estimate of (M^q_{ads}). In the case of charged states, the estimate of the defect formation energies requires some correction terms to align the electrostatic potentials and, then the VBM of different supercells, as described in Ref. [9]. These terms are estimated here but not shown in the above expression for sake of simplicity. Moreover, the presence of a compensating uniform background has been assumed to treat the $G = 0$ term in the total energy of charged supercells. A transition energy level $\varepsilon^{n/n+1}(M_{\mathrm{ads}})$ is defined as the Fermi-level position where the charge states n and $n + 1$ of an M_{ads} molecule have equal formation energy, that is, the Fermi level where both charge states exist and an electronic transition at the level induced by the molecule in the energy gap can occur. Transition energy levels can be observed in experiments where the final charge state relaxes to its equilibrium configuration after the transition. Moreover, transition energy levels permit one to estimate the predominant charge state of an adsorbed molecule at a given value of the Fermi energy, that is, its donor or acceptor character. These levels must be compared to the band energy gap E_{g}, estimated here as the difference between the electron affinity and the ionization potential calculated for the perfect surface. Such an approach permits to compare consistent results. Present estimate of E_{g} is 2.89 eV, to be compared with an experimental value of 3.28 eV [21].

A finite-difference calculation method has been used to estimate the vibrational frequencies (in the harmonic approximation) related to the topmost layers of the molecule–surface system. Such a procedure has been used to estimate the vibrational frequencies of neutral and charges surface species surrounded by water molecules, which are discussed in the following sections. In the present study, these vibrational frequencies have been investigated also by performing *ab initio* molecular dynamics (AIMD) calculations [22]. The supercells used for these calculations have been obtained by adding ≈ 7 Å of empty space to a bulk 48-atom supercell containing four (2 × 2) atomic layers. These supercells include the investigated surface groups embedded in a bilayer of water molecules [23]. AIMD simulations have been performed by using a 3 a.u. time step and a 300 K temperature controlled by Nosé thermostats for about 10 ps. The vibrational frequencies of the investigated systems have been obtained by calculating power spectra from the velocity autocorrelation functions. Such a procedure permits an accurate sampling of the system configurations as well as a better simulation of the experimental conditions.

All calculations have been performed by using the CPMD [24] and the quantum-ESPRESSO packages [25].

3. Results

3.1. O_2 peroxo and hydroperoxo groups

The properties of charged O_2-derived intermediates will be discussed in the following by comparing present LSD results

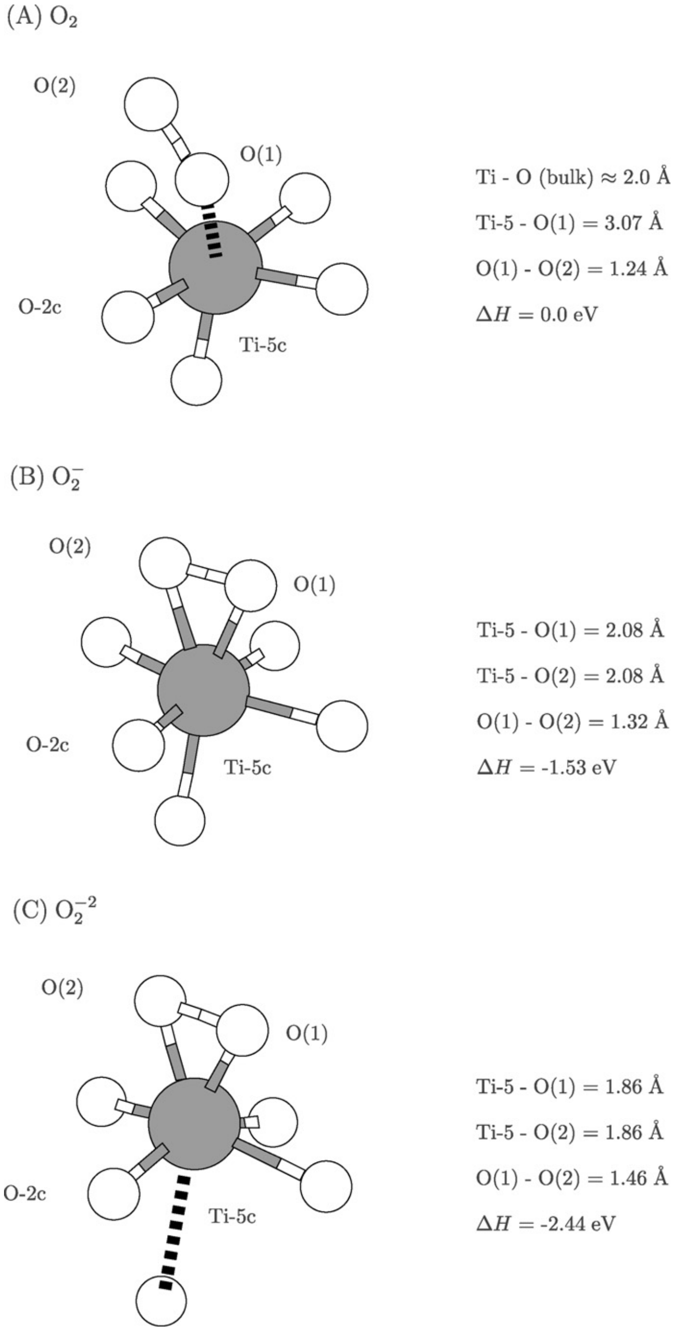

Fig. 2. Optimized geometries and desorption enthalpies estimated by LSD calculations for: (A) O_2 molecule, (B) O_2^{-}, and (C) O_2^{2-} molecules on a surface fivefold-coordinated Ti site. O_2^{-} and O_2^{2-} correspond to surface peroxo species.

with the previous LDA ones [8]. First, we will briefly recall the previous results. The minimum energy configuration for an O_2 molecule corresponds to a molecule located upon a fivefold coordinated Ti^{4+} surface ion, in a configuration similar to that shown in Fig. 2(A). The O_2 molecule weakly binds to the Ti ion as shown by a desorption enthalpy $\Delta H_{des}(O_2)$ of −0.34 eV (hereafter, negative Δ-quantities, enthalpies or energies, indicate endothermic processes) and Ti–O bond distances of 2.31 and 3.19 Å to be compared with Ti–O distances of about 2.0 Å in the anatase bulk. The O_2 molecule induces an occupied and an empty states in the anatase energy gap corresponding to electronic eigenvalues located at 0.60 and 0.89 eV above VBM, respectively. The latter electronic state suggests an acceptor behavior of the adsorbed molecule. The properties of the O_2^- and O_2^{2-} ion-molecules adsorbed at the same Ti site have been therefore investigated. The equilibrium geometries found for these two ion-molecules are similar to those given by LSD calculations, see Fig. 2(B) and (C). The corresponding $\Delta H_{des}(O_2^-)$ and $\Delta H_{des}(O_2^{2-})$ are equal to −1.49 eV and −2.37 eV, respectively. Transition levels $\varepsilon^{0/-1}$ and $\varepsilon^{-1/-2}$ located at 0.92 and 1.44 eV from VBM, respectively, have been estimated by using the $\Omega(O_2^0)$, $\Omega(O_2^-)$, and $\Omega(O_2^{2-})$ formation energies. This result confirms that an adsorbed O_2 molecule induces an acceptor electronic level in the energy gap, which can be doubly occupied.

The results of present LSD calculations closely parallel previous LDA results for what concerns the structural and vibrational properties of the O_2^- and O_2^{2-} surface species as well as the features of their chemical bonds. On the other hand, LSD methods give some different results in the case of the neutral O_2 molecule as well as of the electronic properties. In the former case, the neutral O_2 molecule does not tend to stick to the surface. A $\Delta H_{des}(O_2)$ close to zero is found for a molecule located at different distances from the surface. Moreover, the electronic eigenvalues calculated for a molecule far from the surface show two HOMO's (highest occupied molecular orbitals) corresponding, as expected, to two electrons with parallel spin which are located in the valence band, and two LUMO's (lowest unoccupied molecular orbitals) located in the energy gap close to the conduction band, see Fig. 3. Interestingly, when the O_2 molecule is close to the surface (Ti–O distance equal about to 2.2 Å), there is a lowering and a splitting of the two LUMO's, the lowest one being located at about 1 eV above the VBM, see Fig. 3. This suggests an acceptor character of an O_2 molecule approaching the surface. The evolution of the electronic structure found for O_2^- and O_2^{2-} ion-molecules adsorbed on the surface is shown in Fig. 3. Such a structure confirms the acceptor character of the O_2 molecule suggested by LDA calculations. On the other hand, LSD results give different estimates of the $\varepsilon^{0/-1}$ and $\varepsilon^{-1/-2}$, equal to 1.82 and 2.14 eV, respectively, at variance with LDA results. Altogether, the LSD results substantially confirm the theoretical picture given by the LDA calculations, although introducing some peculiar, yet significant, differences. In fact, by taking into account that the charge on the adsorbed O_2 molecule depends on the position of the Fermi level, LDA results suggest that a strong p-type doping (Fermi level located below the transition level at 0.92 eV) would favor a neutral superoxo-like configuration similar to that shown in Fig. 2(A). On the contrary, such a configuration is not stable in the LSD picture. Moreover, in the case of the non-intentionally doped anatase (Fermi level close to $E_g/2$, i.e., above the transition level at 0.92 eV), LDA result suggest the formation of O_2^- even in the dark, while such a process is unlikely in the LSD picture due to an $\varepsilon^{0/-1}$ equal to 1.82 eV. LDA and LSD agree instead on the fact that an n-type doping or illumination will favor an electron transfer from the surface to the O_2 molecule. Both approaches also describe the O_2 molecule as a strong deep acceptor, thus suggesting that the electrons occupying the corresponding acceptor level are mainly localized on the molecule itself. This is confirmed by plots of charge density distribution (not shown here) and by the dramatic changes of geometry and chemical bonding observed when going from the neutral to the charged molecules. In the O_2^- and O_2^{2-} ion-molecules, the two oxygen atoms are indeed both bonded to a Ti atom in a symmetric configuration, see Fig. 2(B) and (C) and compare with Fig. 2(A), thus forming charged peroxo groups, $Ti(O_2^{2-})$. In these charged groups, the Ti–O distances are close to those in the bulk anatase, thus indicating the formation of strong Ti–O bonds also confirmed by the large desorption enthalpies $\Delta H_{(des)}(O_2^-)$ and $\Delta H_{(des)}(O_2^{2-})$, estimated from both LDA and LSD calculations. LDA and LSD approaches give also similar results for the O_2^- and O_2^{2-} vibrational frequencies as estimated in the harmonic approximation. Thus, previous LDA and present LSD results give the following indications regarding the O_2 surface groups. First, in the conventional model of the TiO_2 chemical bonding, a sixfold coordinated Ti^{4+} ion is surrounded by O^{2-} ions. Present results indicate therefore that under illumination an O_2^{2-} ion-molecule can behave similarly to a bulk O^{2-} ion by (over-)saturating a fivefold coordinated Ti surface atom. Second, the strong, deep acceptor character of the adsorbed O_2 molecule gives, for the first time, a clear theoretical explanation of the electron scavenger behavior of O_2 molecules suggested by the experiments [4,6,7,26,27]. Third, the location of the acceptor level induced by the O_2 molecule as estimated in the LSD approach suggests a massive production of charged $Ti(O_2^{2-})$ peroxo groups only upon UV irradiation. Fourth, a vibrational line at 943 cm^{-1} has been observed in the MIRIR study and assigned to the surface $Ti(O_2)$

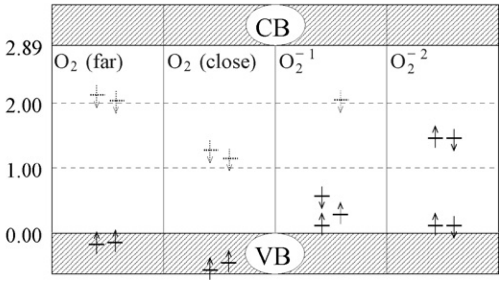

Fig. 3. Location in the anatase energy gap of the LSD electronic eigenvalues (eV) calculated for (from left to right) a neutral O_2 molecule far from the surface, a neutral O_2 molecule close to the surface, and the O_2^- and O_2^{2-} molecules adsorbed on the surface. VB and CB stand for valence and conduction bands, respectively.

peroxo group reported in the path A of Fig. 1. The O–O stretching frequencies estimated here for the different charges of an adsorbed O_2 molecule show that only that corresponding to the charged $Ti(O_2^{2-})$ peroxo group, 950 cm^{-1}, closely agrees with the experiment. This confirms a surface–molecule charge transfer that directly involves the oxygen atoms of the $Ti(O_2^{2-})$ group, as also shown by an O–O bond distance larger than the one of the neutral Ti–OO superoxo-like configuration (see Fig. 2(A)), thus following the trend found for the free O_2 (1.24 Å) and O_2^{2-} (1.34 Å) molecules in the vacuum. All of these results confirm that charged intermediates play a key role in the O_2 photoreduction as already suggested by previous LDA results. Present results confirm also significant changes of the reaction pathways proposed in the MIRIR study. In detail, the reaction path A in Fig. 1 considers that, as a first step, an electron is captured by a Ti^{4+} ion interacting with an O_2 molecule by leading to a superoxo-like species. Then, a second electron is captured to form a (neutral) $Ti(O_2)$ peroxo group. On the contrary, present results indicate that no superoxo species form and both the first and second electrons are captured by the O_2 molecule by forming $Ti(O_2^{1-})$ and $Ti(O_2^{2-})$ peroxo groups, respectively. The above results also suggest that adsorbed O_2^- and O_2^{2-} ion-molecules are hardly detached from the surface, thus questioning the mechanism proposed in the path B of Fig. 1. Finally, in water solutions, the negatively charged $Ti(O_2^{2-})$ peroxo group proposed here favors a reaction with H^+ ion to form surface-bound hydroperoxo groups, Ti–OOH, also suggested by the reaction paths of Fig. 1.

In the case of hydroperoxo groups, once more present LSD results almost parallel previous LDA findings with respect to the structural and vibrational properties and the chemical bonding. On the other hand, LSD results regarding the electronic structure of hydroperoxo groups differ from the LDA results similarly to the case of O_2 intermediates. In detail, in the case of neutral Ti–OOH group, a minimum energy configuration is given by LDA and LSD calculations similar to that shown in Fig. 4(A) for the corresponding charged $Ti–OOH^-$ group.

The electronic structure of the neutral Ti–OOH group is characterized by a half-occupied electronic level in the energy gap found at 0.16 eV from VBM by LDA. In the LSD approach, such an electronic level evolves in a HOMO level located at 0.40 eV and in a LUMO at 1.89 eV from VBM. Regarding the structure of a negatively charged $Ti–OOH^-$ group, the results of LSD and LDA approaches are quite similar and correspond to an equilibrium geometry (see Fig. 4(A)) characterized by a short Ti–O distance. The $Ti–OOH^-$ ion is therefore tightly bonded to the surface as supported by $\Delta H_{(des)}(OOH^-)$ values of −2.09 and −2.17 eV as given by LDA and LSD calculations, respectively. The formation energies of the Ti–OOH and $Ti–OOH^-$ absorbed species give a transition level $\varepsilon^{0/-1}$ located at 0.87 and 1.65 eV above VBM in the cases of LDA and LSD approaches, respectively. This result confirms the acceptor character of the adsorbed OOH group and indicates that it will be negatively charged only upon illumination, thus behaving like an adsorbed O_2 molecule. A further similarity with the O_2 molecule concerns the nature of the charge transfer. The surface $Ti–OOH^-$ group is characterized indeed by an O–O bond distance close to that found for a free OOH^- ion (1.49 Å), thus showing that the charge transfer involves once more the O atoms of the group in place of the involved Ti^{4+} ion.

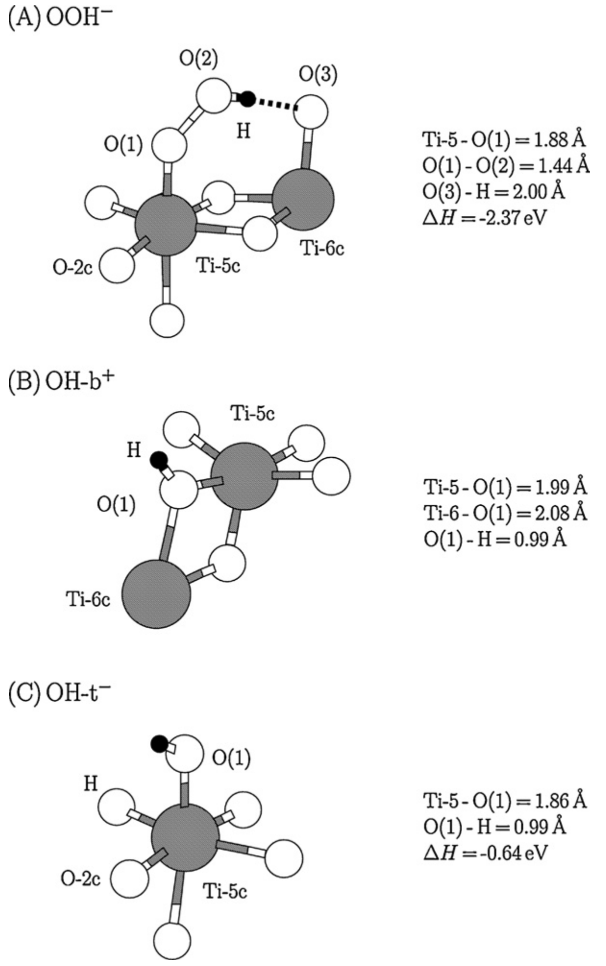

Fig. 4. Optimized geometries and desorption enthalpies estimated by LSD and LDA + U calculations for: (A) an adsorbed OOH^- group; (B) an OH-b^+ bridging hydroxyl group; and (C) an OH-t^- terminal hydroxyl group.

Finally, both LDA and LSD results indicate that the presence of surrounding water molecules has significant effects on the properties of the Ti–OOH and $Ti–OOH^-$ species. In the case of surface $Ti–OOH^-$, the water molecules induce only a rearrangement of its structure. On the contrary, in presence of water molecules, the Ti–OOH is unstable, it loses its H atom by forming a H_3O^+ ion and a surface O_2^- peroxo species. This is a significant result because it indicates that $OOH^\bullet$ radicals should not be released by the anatase surface in contact with aqueous solutions. The O–O stretching frequency estimated for the $Ti–OOH^-$ group, 963 cm^{-1}, can contribute to the experimental line of 943 cm^{-1} cited above. The estimated H bending frequency, 1154 cm^{-1}, contributes to the experimental band reported at 1250–1120 cm^{-1}. Present results agree therefore with the formation of surface hydroperoxo groups suggested in the MIRIR study and confirm that these groups should be negatively charged.

The results achieved for the hydroperoxo groups confirm the importance of charged intermediates in the O_2 photoreduction processes already suggested by LDA findings. Charged Ti–OOH$^-$ groups can be formed indeed by a direct reaction of Ti(O_2^{2-}) peroxo groups with H^+ ions. In turn, charged Ti–OOH$^-$ groups should easily react with a further H^+ ion by forming H_2O_2 molecules. The charged intermediates proposed here suggest a revision of the reaction path A of Fig. 1 as well as the existence of an efficient protonation process leading to the formation of H_2O_2 molecules.

On the other hand, the vibrational frequencies estimated for hydroperoxo radicals surrounded by water molecules do not agree with the results of the MIRIR study. This result together with the unlikely detachment of O_2^{1-} groups from the surface and the instability of the Ti–OOH groups mentioned above induce to rule out the path B of Fig. 1 in a full agreement with previous LDA results.

3.2. Surface OH groups

A bridge OH group (OH-b) is a twofold coordinated OH group involving a surface O-bridge atom and characterized by a structure very similar to that shown in Fig. 4(B) for the charged OH-b$^+$ group. A recent theoretical study has investigated the properties of OH-b groups by using hybrid exchange functionals and suggested that localized Ti^{3+} 3d states are introduced by these surface groups at variance with the results given by an LDA–PBE approach [13]. Such an issue is presently under investigation in our group. Preliminary results show that an LDA + U approach can reproduce the results achieved by hybrid exchange functionals. Thus, we have used such an approach to reinvestigate the properties of an isolated OH-b group. Quite interestingly, in the case of an isolated OH-b group on the anatase surface, our LDA + U results do not show significant differences from those found by using an LDA–PBE approach [8]. Thus, in the following, we rediscuss the LDA–PBE results by focusing on charge transfer processes and vibrational properties. First, the similar structures of the OH-b and charged OH-b$^+$ groups contrast with the strong structural rearrangement found in the case of the charged and neutral states of both the O_2 molecules and (Ti)–OOH groups. This suggests that a charge transfer does not directly involve the OH-b group. The electronic structure of the neutral OH-b group is characterized by a half-occupied electronic level located at 0.13 eV below the conduction band minimum (CBm), which suggests a donor behavior of this group. The properties of the positively charged OH-b$^+$ have been therefore investigated. In particular, an $\varepsilon^{+1/0}$ transition level located at 0.75 eV below the CBm has been estimated from the (OH-b^0) and (OH-b^{1+}) formation energies. This result confirms the donor character of the OH-b group. However, it also indicates that this group behaves as a rather deep donor at variance with the above electronic eigenvalue which suggests a typical shallow behavior. Notwithstanding, plots of the electronic charge density corresponding to the OH-b level (not shown here) indicate that the unpaired electron is delocalized on a few Ti surface atoms in the case of an isolated OH-b group. The OH-b group will be positively charged when the Fermi level is located close to the midgap. Present results account therefore for the electron trapping character often attributed to these surface groups [6].

The formation of OH-b groups has not been considered in the MIRIR study. On the contrary, present results show that a surface OH-b surrounded by water molecules is characterized by two H bending frequencies at 1014 and 1075 cm^{-1} which can contribute to an experimental 1023 cm^{-1} band. Alternatively, the 1075 cm^{-1} mode can contribute to the 1250–1120 cm^{-1} experimental band cited above. Present results suggest therefore that OH-b groups may form at the low pH values characterizing the experimental conditions of the MIRIR study, which favor the capture of H^+ ions by surface bridging O atoms.

Terminal OH surface groups having the O atom bonded to a Ti surface atom, OH-t, have been indicated in the reaction paths of Fig. 1, although they were not discussed in the MIRIR study. The electronic structure of the neutral OH-t group is characterized by a half-occupied electronic level inside the valence band. Further peculiarities of this group are that: (i) the same electronic structure is found for an OH group located in the vacuum far from the surface and, (ii) a same geometry is found for the neutral OH-t and the charged OH-t^{-1} groups. This geometry is characterized by a short O–Ti distance of 1.85 Å, which indicates the formation of a quite strong Ti–O bond. These results suggest that an OH group can be bonded to a surface Ti^{4+} ion only in the negatively charged state. In this case, the OH-t^{-1} group behaves similarly to an O^{2-} ion of the bulk TiO_2 by recovering a sixfold coordination for the involved Ti^{4+} ion. A comparison of the vibrational frequencies calculated for the charged OH-t^{-1} groups with those of the MIRIR study shows that the calculated frequencies have no experimental counterparts at high values of pH where these groups should be strongly favored. This result suggests that OH-t surface groups do not play a significant role in the O_2 photoreduction and should be removed from the reaction paths of Fig. 1. On the other hand, the absence of charged OH-t^{-1} groups in presence of alkaline solutions is quite surprising. This problem is currently under investigation in our group.

3.3. Vibrational frequencies from AIMD

AIMD simulations have been performed for a system including the anatase surface, an OH-b group, a Ti–OOH group and a bilayer of water molecules [23]. The presence of those two surface species in the same supercell induces a donor–acceptor compensation, which leads to the formation of the ionized OH-b$^+$ and Ti–OOH$^-$ groups. These AIMD simulations have been performed to validate the results achieved by the finite-difference calculations against the effects of temperature and hydrogen bonds formed with the surrounding water molecules. Such an investigation has been performed on the OH-b$^+$ and Ti–OOH$^-$ groups because the finite-difference calculations show that the relative H vibrational modes are strongly sensitive to the effects of hydrogen bonds. In turn, these effects can be affected by the temperature, which is kept at the value of 300 K in the AIMD simulations. Fig. 5 reports a

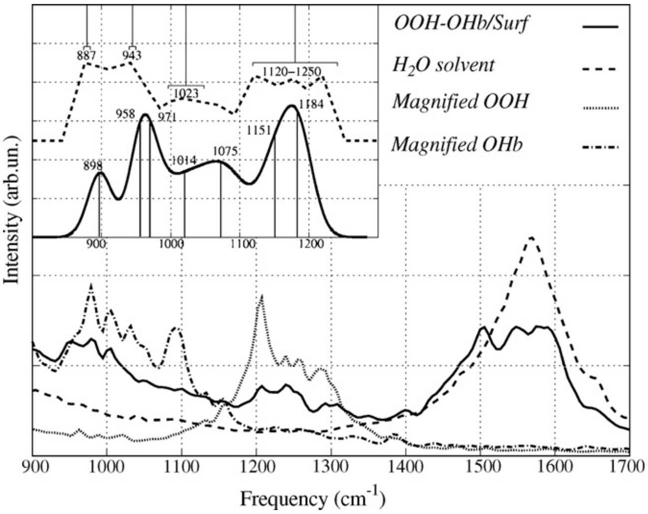

Fig. 5. The vibrational spectrum of an OH-b^+ and Ti–OOH^- groups surrounded by water molecules is reported in the figure together with the one of water molecules in contact with the anatase surface and the magnified contributions of the two surface groups. The spectra have been obtained by AIMD calculations. The inset to the figure shows a theoretical simulation of the experimental spectrum, as previously reported in Ref. [8] (solid line), within a faithful representation of the experimental spectrum itself, shown in Ref. [7] (dashed line). Theoretical frequency values not discussed in text, namely 898 and 1184 cm^{-1}, have been assigned to hydrogen peroxide stretching and bending modes, respectively, both in Ref. [7] (experimental lines at 887 and 1120–1250 cm^{-1}) and Ref. [8].

plot of the vibrational spectra of the system described above and, for comparison, of a system including only water molecules. This figure also reports magnifications of the contributions of the two surface groups to the vibrational spectrum. The achieved results are in a very close agreement with those produced by finite-difference calculations performed in the LDA approach, and shown in the inset to Fig. 5. In the case of the OH-b^+ group, vibrational frequencies are found close to 1000 and 1100 cm^{-1} to be compared with the values of 1014 and 1075 cm^{-1}, respectively. A H bending mode close to 1200 cm^{-1}, and a weak O–O stretching mode (which is clearly appreciable in a plot of the spectrum in a logarithmic scale, not shown here) are found for the Ti–OOH^- group, which also agree with the 971 and 1151 cm^{-1} lines produced by the finite-difference calculations. Finally, the H bending modes of the water molecules are close to 1600 cm^{-1} in a good agreement with the experimental values reported in the MIRIR study. The results produced by finite-difference calculations, achieved for a system at a 0 K temperature, have stressed the importance of H bonds formed by surface groups with water molecules [8]. The AIMD results fully confirm the importance of such H bond effects even at room temperature.

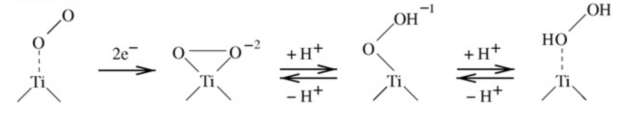

Fig. 6. Reaction pathway for the O_2 photoreduction as proposed in the present study.

4. Conclusions

Present LSD and LDA + U results confirm the key role of charged intermediates in the O_2 photoreduction already suggested by previous LDA results. Generally, LSD results closely parallel previous LDA results for what concerns the structural and vibrational properties of the O_2^- and O_2^{2-} surface species as well as the features of their chemical bonds. Some differences are found instead for the neutral O_2 molecule and the electronic properties. Superoxo-like configurations are predicted to be unstable. Moreover, in the case of the non-intentionally doped anatase, LDA result suggest the formation of Ti(O_2^-) even in the dark, while such a process is unlikely in the LSD picture. Both LDA and LSD results indicate that an n-type doping or illumination will favor an electron transfer from the surface to the O_2 molecule and describe the O_2 molecule as a strong deep acceptor, thus suggesting that the electrons occupying the corresponding acceptor levels are mainly localized on the molecule itself. This strong, acceptor character gives a clear theoretical explanation of the electron scavenger behavior of O_2 molecules suggested by the experiment. Moreover, present results indicate that a surface–molecule charge transfer piles up electronic charge on the O atoms of the O_2 molecule by leading to the formation of charged peroxo intermediates strongly bonded to a Ti atom. These results imply that charged intermediates have relevant effects on the proposed reaction pathways as also suggested by previous LDA results. The deep acceptor character of an adsorbed O_2 molecule suggests a massive production of charged Ti(O_2^{2-}) peroxo groups upon UV irradiation. The negative charge of these intermediates favors the reaction with H^+ ions to form hydroperoxo groups. Even these intermediates behave as deep acceptors, thus being negatively charged under illumination. They can easily capture therefore further H^+ ions to form H_2O_2 molecules. All together, these results indicate that the reaction path A of Fig. 1, revised as schematized in Fig. 6, supports the existence of an efficient protonation process leading to the formation of H_2O_2 molecules. Present LDA + U results also parallel LDA–PBE results and indicate that OH-b donors can be favored by low pH values. The present theoretical picture, based on charged intermediates, is supported by the fact that only the vibrational frequencies estimated for charged species agree with the experimental lines. Finally, the results produced by AIMD calculations confirm the importance of the H bonds formed by H-containing intermediates with surrounding water molecules suggested by finite-difference calculations.

Acknowledgement

The authors thank P. Giannozzi for helpful discussion and comments.

References

[1] M.R. Hoffmann, S.T. Martin, W. Choi, D.W. Bahnemann, Chem. Rev. 95 (1995) 69.
[2] A.L. Linsebigler, G. Lu, J.T. Yates Jr., Chem. Rev. 95 (1995) 735.

[3] A. Mills, S. Le Hunte, J. Photochem. Photobiol. A 108 (1997) 1.
[4] A. Fujishima, T.N. Rao, D.A. Tryk, J. Photochem. Photobiol. C 1 (2000) 1.
[5] U. Diebold, Surf. Sci. Rep. 48 (2003) 53.
[6] O. Carp, C.L. Huisman, A. Reller, Prog. Solid State Chem. 32 (2004) 33.
[7] R. Nakamura, A. Imanishi, K. Murakoshi, Y. Nakato, J. Am. Chem. Soc. 125 (2003) 7443.
[8] G. Mattioli, F. Filippone, A. Amore Bonapasta, J. Am. Chem. Soc. 128 (2006) 13772.
[9] C.G. Van de Walle, J. Neugebauer, J. Appl. Phys. 95 (2004) 3851.
[10] A. Amore Bonapasta, F. Filippone, Surf. Sci. 577 (2005) 59.
[11] M. Lazzeri, A. Vittadini, A. Selloni, Phys. Rev. B 63 (2001) 155409.
[12] M. Cococcioni, S. de Gironcoli, Phys. Rev. B 71 (2005) 035105.
[13] C. Di Valentin, G. Pacchioni, A. Selloni, Phys. Rev. Lett. 97 (2006) 166803.
[14] P. Hohenberg, W. Kohn, Phys. Rev. 136 (1964) B864.
[15] W. Kohn, L.J. Sham, Phys. Rev. 140 (1965) A1133.
[16] J.P. Perdew, K. Burke, M. Ernzerhof, Phys. Rev. B 77 (1996) 3865.
[17] D. Vanderbilt, Phys. Rev. B 41 (1990) 7892.
[18] K. Laasonen, A. Pasquarello, C. Lee, R. Car, D. Vanderbilt, Phys. Rev. B 47 (1993) 10142.
[19] A. Amore Bonapasta, F. Filippone, P. Giannozzi, M. Capizzi, A. Polimeni, Phys. Rev. Lett. 89 (2002) 216401.
[20] C.G. Van de Walle, J. Neugebauer, Nature 423 (2003) 626.
[21] L. Forro, D. Chauvet, L. Emin, L. Zuppiroli, H. Berger, F. Levy, J. Appl. Phys. 75 (1994) 633.
[22] R. Car, M. Parrinello, Phys. Rev. Lett. 55 (1985) 2471.
[23] A. Tilocca, A. Selloni, J. Chem. Phys. 119 (2003) 7445.
[24] CPMD V3.9 Copyright IBM Corp 1990-2005, Copyright MPI fuer Festkoerperforschung Stuttgart 1997-2001, http://www.cpmd.org.
[25] S. Baroni, A. Dal Corso, S. de Gironcoli, P. Giannozzi, C. Cavazzoni, G. Ballabio, S. Scandolo, G. Chiarotti, P. Focher, A. Pasquarello, K. Laasonen, A. Trave, R. Car, N. Marzari, A. Kokalj, http://www.pwscf.org/.
[26] R. Nakamura, Y. Nakato, J. Am. Chem. Soc. 126 (2004) 1290.
[27] T. Zubkhov, D. Stahl, T.L. Thompson, D. Panayotov, O. Diwald, J.T. Yates Jr., J. Phys. Chem. B 109 (2005) 15454.